

In Silico Study of Chemical Compounds in *Plantago major* L. as Anti-Androgen

Achmad Al Baihaqi^{1*}, Hasna Siti Munifah Isman¹, Ganis Fitria Fauziyyah¹,
Rismauli Ruth Natasari Hutabarat¹, Adi Hartono¹, Sandra Megantara²

¹Undergraduate Program in Pharmacy, Faculty of Pharmacy, University of Padjadjaran, West Java, Indonesia 45363.

²Department of Pharmaceutical Analysis and Medicinal Chemistry, Faculty of Pharmacy, University of Padjadjaran, West Java, Indonesia 45363.

Abstract

Prostate cancer is the most common type of cancer diagnosed in men worldwide and the second leading cause of death after lung cancer. Testosterone and dihydrotestosterone (DHT) have been known to play an essential role in prostate cancer. Androgen receptor (AR) binding to the ligand allows homodimerization and translocation to the nucleus, which acts as a transcription factor for androgen-responsive genes such as PSA (Prostate-specific antigen). Although many anti-androgens have been established, including Bicalutamide, Flutamide, and Abiraterone, the problem of non-specific cytotoxicity effects and cancer recurrence due to potential drug resistance remains a significant obstacle to establishing effective therapy. *Plantago major* L. is one of the plants that can choose anticancer therapy because, based on reports, it has anticancer activity through DNA damage in cancer cells. This study focused on the search for the potential phytochemical activity of *Plantago major* L. as an anti-androgen, non-cytotoxic, and had significant AR inhibitory activity. This study uses Lipinski prediction (RO5), ADMET prediction, and a structure-based approach with molecular docking techniques using the PDB ID 2AM9 receptor structure and 13 compounds from *Plantago major* L. as test ligands compared to known AR antagonists. From the research results, Hispidulin has the highest potential as an anti-androgen with binding energy (-9.43 kcal/mol) that is closest to natural ligands and is smaller than Flutamide as a comparison drug. This anti-androgen activity was hypothesized from the similarity of hydrogen bonds with amino acid residues 705-Asn and 711-Gln as key AR residues present in Hispidulin.

Keywords: Prostate cancer, Androgen Receptor, *Plantago major* L., ADMET, *In Silico*.

INTRODUCTION

Cancer is a group of diseases in which body cells grow uncontrollably and can metastasize from one part of the body to another (Moradi, Khakzad Kelarijani, and Shokri, 2021). Cancer is the second leading cause of death worldwide. Based on Globocan 2020, it is estimated that it will account

for 19.3 million new cancer cases and nearly 10 million deaths by 2020 (Sung, *et al.*, 2021). One of the cancers that are included in the top ten, with the

Submitted: January 1, 2022

Revised: May 12, 2022

Accepted: May 13, 2022

*Corresponding author: achmad18002@mail.unpad.ac.id

highest number of new cases and deaths in 2020, is prostate cancer (WHO, 2021b).

Prostate cancer is the most common type of cancer in men worldwide and the second leading cause of death after lung cancer (Siegel, *et al.*, 2021). By 2020 in terms of new cases, prostate cancer is estimated to account for 1.41 million cases (WHO, 2021b). In Indonesia, in 2020, the total number of new cases of prostate cancer in men reached 7.4%, with a total incidence of 11.6 and 4.5 deaths based on age-standardised rate (world) per 100,000 (WHO, 2021a). The incidence of prostate cancer has been associated with various risk factors such as age (30-40 years), genetic factors, lifestyle, and environmental factors (Moradi, Khakzad Kelarijani and Shokri, 2021). The cancer burden continues to grow globally, estimated to be 28.4 million by 2040, 47% from 2020, making low- and middle-income countries the least prepared to manage this burden due to limited access to diagnosis and treatment (Sung, *et al.*, 2021).

It is well known that natural androgens, such as testosterone and dihydrotestosterone (DHT), play an essential role in prostate cancer, especially castration-resistant prostate cancer (CRPC). CRPC often metastasizes and responsible for most prostate cancer-related deaths (Rice, Malhotra, and Stoyanova, 2019). Androgen Receptor (AR) is a member of the nuclear receptor superfamily and has a structure similar to the estrogen receptor, progesterone receptor, glucocorticoid receptor, and thyroid hormone receptor, acting as a steroid receptor transcription factor for testosterone and dihydrotestosterone. This receptor has four main domain namely N-terminal, DNA binding domain, hinge region, and ligand-binding domain (LBD) (Fujita and Nonomura, 2019). DHT binds to the ligand-binding domain region which is then followed by a change in the AR conformation (Fujita and Nonomura, 2019), DHT binds to AR separates chaperone proteins (HSP27 and HSP70). Ligand-bound ARs allow homodimerization and translocation to the nucleus. They attach to androgen

response elements (AREs) and act as transcription factors for androgen-responsive genes such as PSA and others (Scher and Sawyers, 2005).

Although many anti-androgens have been established, including Bicalutamide, Flutamide, and Abiraterone, the problem of non-specific cytotoxicity effects and cancer recurrence due to potential drug resistance remains a significant obstacle to establishing effective therapy (Peng, *et al.*, 2019; Tsao, *et al.*, 2019). Plants can be an alternative therapy option in the treatment of cancer. Several researchers report that natural products have the minimum potential for safety and side effects. One plant that has the potential as an alternative cancer therapy is *Plantago major* L. *Plantago major* L. has been reported to have anticancer activity through DNA damage in cancer cells (Kartini, *et al.*, 2017).

Plantago major L. as spoon leaf in local Indonesian name is a herbaceous plant belonging to the Plantaginaceae tribe. This plant is widely distributed globally, with more than 275 species have been reported (Kartini, *et al.*, 2017). This plant grows wild as a weed in tea and rubber plantations (BPOM, 2010). *Plantago major* L. is a plant rich in secondary metabolites. *Plantago major* L. contains several effective phytochemicals such as flavonoids, terpenoids, alkaloids, caffeic acid derivatives, iridoid glycosides, polysaccharides, fats, vitamins, and organic acids to the therapeutic effect. For thousands of years in Asian traditional medicine, *Plantago major* L. has been used as a powerful non-toxic therapeutic agent in inhibiting inflammation. *Plantago major* L. is efficacious as a wound healer, anti ulcerative, antidiabetic, antidiarrheal, anti-inflammatory, antinociceptive, antibacterial, and antiviral agent. In addition, *Plantago major* L. contains antioxidants and free radical scavengers that can combat fatigue and cancer (Adom, *et al.*, 2017).

Based on *in vitro* studies, ethanol extract of *Plantago major* L. leaf with various temperatures (hot and cold) showed anticancer activity on Acute

Myeloblastic Leukemia (AML) cells. *Plantago major* L. leaf ethanol extract had the most significant effect on tumor cell inhibition 74%, followed by *Plantago major* L. leaf hot water extract 54.6% (Mohamed, *et al.*, 2011). In another study, methanol and aqueous extracts of *Plantago major* L. showed the most significant antiproliferative activity compared to other plants with IC_{50} values between 153.38 and 247.41 g/mL. Breast and prostate cancer are closely related because tumor development and growth depend on androgen receptor (AR) expression (Sak, 2014). The aqueous extract of the *Plantago major* L. seed was reported has antiproliferative activity against the KB, MCF-7, MDA-MB-231, and A549 cell lines (Kartini, *et al.*, 2017).

In addition, *Plantago major* L. was reported to have low toxicity with an LD_{50} value of 1 g/kg BW rats given by intraperitoneal injection, while orally >4 g/kg BW (BPOM, 2010). Therefore, *Plantago major* L. can be developed as an alternative cancer therapy in the future. This study focused on the search for the potential phytochemical activity of spoon leaf as an anti-androgen that show cytotoxicity and had significant AR inhibitory activity. This

study uses Lipinski (RO5) and ADMET predictions in a structure-based approach by molecular docking techniques.

METHOD AND MATERIALS

The hardware used is a personal computer with AMD A4-9125 Radeon R3, 4 Compute Cores 2C + 2G @ 2.30 GHz 4 GB RAM and is operated by Windows 10 Home 64-bit. This research uses software including ChemDraw 19.0 and Chem3D 19.0, AutoDock 4.2.6, and AutoDockTools 1.5.6 from The Scripps Research Institute, BIOVIA Discovery Studio 2021, SwissADME website (<http://www.swissadme.ch/>) for prediction of Lipinski rules (RO5), and sites (pkCSM, Admetlab, Protox-II) for the prediction of ADMET (HIA, Caco-2, PPB, BBB, Mutagens, Carcinogens) obtained from the web free of charge.

The materials used in this study consisted of a receptor structure, a test ligand structure, and a reference ligand structure. Androgen Receptor (AR) obtained 3D Receptor Structures from the Protein Data Bank (PDB) (<http://www.rscb.org/>) with PDB ID 2AM9. The test ligands used were

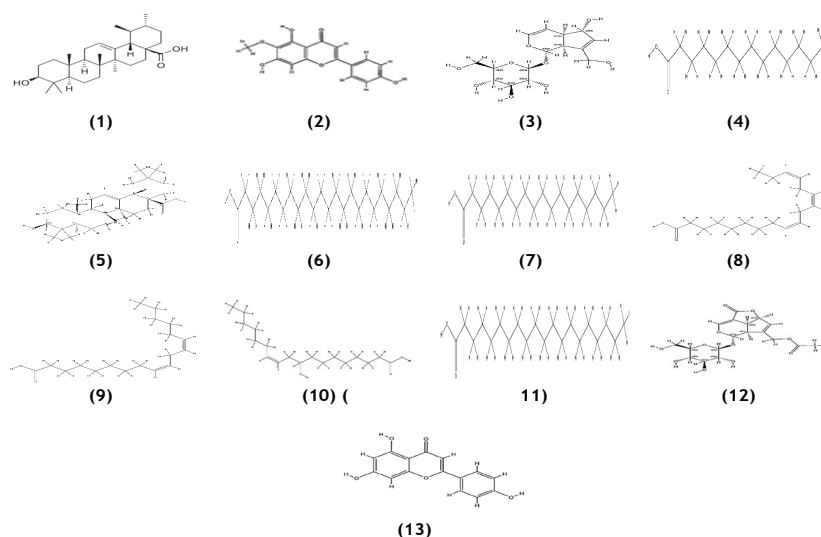


Figure 1. Structure test ligands of compounds in *Plantago major* L. from RO5 screening results and ADMET prediction.

Table 1. Lipinski profile of test compounds.

No	Compounds	Molecular Weight (<500 Da)	Log P (<5)	H-Bond	
				Donor (<5)	Acceptor (<10)
1	Apigenin	270.24	2.11	3	5
2	Aucubin	346.33	-2.07	6	9
3	Myristic Acid	228.37	4.45	1	2
4	Oleanolic Acid	456.7	6.06	2	3
5	Ursolic Acid	456.7	5.88	2	3
6	Hispidulin	300.26	0.22	3	6
7	Lignoceric acid	368.64	8.1	1	2
8	Stearic acid	284.48	5.93	1	2
9	Linolenic acid	278.43	5.09	1	2
10	Linoleic acid	280.45	5.45	1	2
11	9-hydroxy-cis-11-octadecenoic acid	298.46	4.82	2	3
12	Arachidic acid	312.53	6.62	1	2
13	Asperuloside	414.36	-1.33	4	11

13 compounds from spoon leaf (*Plantago major* L.), as shown in Figure 1, consisting of ursolic acid (1); hispidulin (2); aucubin (3); myristic acid (4); oleanolic acid (5); lignoceric acid (6); stearic acid (7); linolenic acid (8); linoleic acid (9); 9-hydroxy-cis-11-octadecenoic acid (10); arachidic acid (11); asperuloside (12); and apigenin (13). The 13 test compounds resulted from screening 43 compounds based on Lipinski's rule (RO5) and ADMET predictions. The Lipinski's parameters used in selecting these 13 compounds were molecular weight less than 500 Da, Log *P* value less than 5, less than five hydrogen bonds donor, and hydrogen bonds acceptor less than 10 (Lipinski, et al., 1997).

The reference ligands used consisted of Bicalutamide, Flutamide, and Abiraterone, which are androgen receptor inhibitors that have been marketed and are commonly used as prostate cancer therapy. The docking simulation was made using the Lamarckian GA genetic algorithm with 100 GA runs. The main parameters observed in this docking simulation are gibs energy (ΔG) and amino acid

interaction residues. Gibbs energy (ΔG) is a marker of binding affinity and residues of amino acid interactions as a marker of interaction (Bronowska, 2011).

RESULTS

Lipinski Prediction (Rule of Five)

The active compound must have the ability to penetrate biological membranes and also have good permeability. To determine the permeability of compounds can be done using a prediction based on Lipinski's rule of five (RO5) (Lipinski, et al., 1997). The test compound should not have a molecular weight of more than 500 Da because it can make it difficult to penetrate the cell membrane. Compounds with a log *P* value greater than 5 indicate that the compound is more lipophilic, which means it will be very tightly bound to the membrane, making it challenging to recognize the target enzyme and toxic. However, a log *P* value that is too small or negative is also not good

because it will be difficult to penetrate the lipid bilayer membrane. At the same time, the hydrogen bonding of the donor and acceptor in the compound indicates the amount of hydrogen bonding capacity. If the hydrogen capacity is higher, the energy required for the absorption process will also be higher. The number of hydrogen bonds for donors in the test compounds allowed is less than 5, while for acceptors, it is less than 10 (Brito and Araújo De Brito, 2011).

The test compounds meet the requirements to form an oral preparation if there is no more than one violation of Lipinski's rules (Lipinski, 2004). As shown in Table 1, all the compounds that continued for the docking process met the requirements of Lipinski's rule. None of the 13 compounds exceeded the deviation requirements specified by Lipinski, which means these compounds have good permeability.

Prediction of Absorption, Distribution, and Toxicity

In silico, ADMET and drug similarity prediction help find new targets and compounds with anticipated biological activity (Cheng, *et al.*, 2012). The active compound must have an excellent pharmacokinetic profile and be non-toxic. Prediction of the ADMET profile of the active compound in this study was carried out through web-based testing. ADMET predictions in this study were designed from compounds that passed RO5. Predictions of ADMET include absorption (HIA, Caco-2), distribution (PPB, BBB), and toxicity (Mutagens, carcinogens).

The absorption profile was predicted using HIA and Caco-2. The predicted distribution profile can be seen in Table 2. Based on the test results, 11 of the 13 test compounds were well absorbed in the intestine (HIA>80%) (Villanueva-Paz, *et al.*, 2021).

Table 2. ADMET profile of test compounds.

Molecule	Absorption		Distribution		Toxicity	
	HIA (%)	Caco-2 (Log unit)	PPB (%)	BBB (Log BB)	Mutagen	Carcinogen
Apigenin	93.25	-4.847	97.255	-0.734	non-mutagen	(-)
Aucubin	35.949	-5.566	16.621	-1.154	non-mutagen	(-)
Myristic Acid	92.691	-4.96	98.201	-0.027	non-mutagen	(-)
Oleanolic Acid	99.931	-5.3	98.632	-0.14	non-mutagen	(+)
Ursolic Acid	100	-5.221	98.843	-0.141	non-mutagen	(+)
Hispidulin	84.654	-4.882	96.962	-1.12	non-mutagen	(-)
Lignoceric Acid	86.693	-5.196	98.901	-0.631	non-mutagen	(-)
Stearic Acid	91.317	-5.068	99.218	-0.195	non-mutagen	(-)
Linolenic Acid	92.836	-4.631	97.119	-0.115	non-mutagen	(-)
Linoleic Acid	92.329	-4.733	98.391	-0.142	non-mutagen	(-)
9-Hydroxy-Cis-11-Octadecenoic Acid	91.862	-4.999	97.543	-0.029	non-mutagen	(-)
Arachidic Acid	90.63	-5.099	99.128	-0.279	non-mutagen	(-)
Asperuloside	51.524	-5.858	20.364	-1.439	non-mutagen	(-)

8 of the 13 test compounds had good permeability (Caco-2 > -5.15 log units). Permeability has a relationship with solubility. Drugs with good permeability and solubility can increase bioavailability (Larregieu and Benet, 2014).

The distribution profile was predicted using PPB (Plasma Protein Binding) and BBB penetration (Blood-Brain Barrier). PPB% level of drug can affect drug action, disposition, and efficacy (Mannhold, 2008). Prediction of distribution profile can be seen in Table 2; 11 of the 13 test compounds were well bound to plasma protein (PPB > 90%). A high PPB has a low volume of distribution. Drugs with low volumes of distribution usually require low doses to reach certain plasma concentrations and have long plasma half-lives. PPB > 99% is not recommended because it can reduce efficacy; the

unbound fraction is usually responsible for the pharmacological activity (Bohnert and Gan, 2013). The test compounds studied were predicted to pass the BBB (log BB > 0.3) easily. It is very useful as a therapeutic agent for metastatic prostate cancer.

The toxicity profile was predicted by assessing mutagenic and carcinogenic properties. All test compounds were predicted to be non-mutagens. However, two compounds, namely oleanolic acid and ursolic acid, are predicted to be carcinogenic. Carcinogenicity can be defined as the ability of a substance to cause cancer (Dieter, 2018). From the prediction results of ADMET, there are 8 compounds as potential drug candidates, including apigenin, myristic acid, hispidulin, stearic acid, linolenic acid, linoleic acid, hydroxy-cis-11-octadecenoic acid, and arachidic acid.

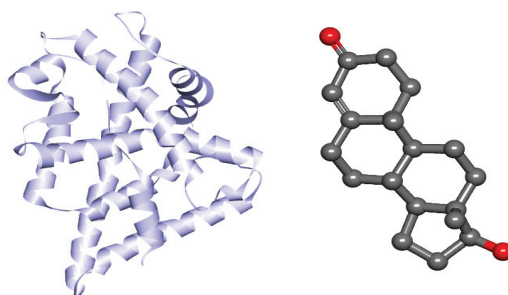


Figure 2. Receptor-Ligand Preparation Results (left: AR(2AM9); right: Testosterone).

Ligand-Receptor Preparation

The structure 3D AR PDB ID 2AM9 was downloaded from the PDB database on the website <https://www.rcsb.org/>. From the download results, 2AM9 was complexed with testosterone (nature ligands) (pereira de Jésus-Tran, *et al.*, 2006). A sulfate ion complex and a water molecule from the 2AM9 receptor complicate the docking process. BIOVIA Discovery Studio 2021 software is beneficial in eliminating this complex (Rendi, *et al.*, 2021). The results of the receptor-natural ligand separation are shown in Figure 2.

After the AR (2AM9) structure has separated from its natural ligand, the receptor structure has no water molecules and becomes a free receptor. The addition of polar hydrogen and Kollman charge

into the file is required to prepare the docking simulation. Since the ligand is not a peptide, the non-polar hydrogen and Gasteiger charges are assigned to the ligand file. The receptor is kept rigid, and the tethered ligand remains flexible in exploring the higher possibility of binding to its receptor in different binding modes. In docking simulations, the target receptor usually acts as a macro-molecule while the ligand acts as a substrate or drug candidate (Gowthaman, Jayakanthan, and Sundar, 2008; Atkovska, *et al.*, 2014). Energy minimization setting before docking is required to get better docking results. Energy minimization aims to find a stable conformer that is structurally close to the initial molecular arrangement, which plays a role in achieving the smallest potential energy conformer

(ΔG Negative). It is considered close to the biological system (Roy, Kar, and Das, 2015).

Redocking

The receptor has a resolution of 1.64 and binds to the natural ligand of testosterone, a steroid hormone known to have agonist action against androgen receptors (Pereira de Jésus-Tran, *et al.*, 2006). The method validation process was carried out through the redocking process of testosterone as a natural ligand extracted from the 2AM9 complex. The grid box size is determined before the ligand is attached to the receptor using the grid parameter. The grid box size used in this study is 40x40x40 (x,y,z), with a range between grid points is 0.375 Å adjusting the size of the ligand.

The redocking or validation process parameters used in this study are grid box coordinates, Root Mean Deviation Square (RMSD), Gibbs free energy (ΔG), and amino acid residue interactions, whose results are listed in Table 3. RMSD is deter-

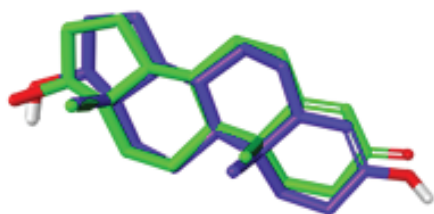


Figure 3. Ligand overlay after redocking (purple) and before redocking (green) on the 2AM9-Testosterone complex.

mined by comparing the positions of ligand atoms experimentally and functions based on prediction algorithms. The flexibility of these ligands can affect the accuracy of the part of the complex formed. This RMSD score explains the average difference in the distance of each atom from the ligand after the redocking process. The small value of RMSD indicates the high validity of the docking method and has similar results that are higher with crystallographic results (Kontoyianni, McClellan and Sokol, 2004; Bissantz, Folkers and Rognan, 2000; Pratama, 2015). An RMSD score of less than 2 indicates a valid docking method (Gowthaman,

Jayakanthan, and Sundar, 2008). The redocking results from this study gave an RMSD score of 0.78, which suggests that the process using the 2AM9 complex can provide valid results for docking purposes.

The Gibbs free energy here is a marker of bond affinity strength, and amino acid residues act as interaction markers, carried out to evaluate the similarity of amino acid interactions which indicate that the test ligand and will have the same activity as natural ligands (Clark and Labute, 2007; Forli, *et al.*, 2016). The results in Table 3 show that there are nine amino acid residue interactions and one hydrogen bond between the androgen receptor and the natural testosterone ligand.

Molecular Docking Simulation

The docking or molecular docking process for all test ligands was carried out in the same steps as the re-docking (validation) phase with the same size and coordinate grid box. Lamarckian genetic algorithm with 100 GA running was used to find the best conformers. The docking parameters observed in this study were the value of Gibbs free energy (ΔG), inhibition constant, hydrogen

Table 3. Result of redocking process.

Parameters	Value
PDB ID	2AM9
Nature ligand	Testosterone
Grid box size (Å)	40x40x40
Grid box coordinate	x=26.907 y=2.557 z=5.181
RMSD (Å)	0.78
ΔG (kcal/mol)	-11.98
Residual amino acids interaction	Hydrogen bond : 711 - Gln,705-Asn Hydrophobic-bonds: 707-Leu, 741-Trp, 745-Met, 742-Met, 704-Leu, 873-Leu, 876-Phe, 780-Met

Table 4. Docking results of test ligands and reference ligands against AR (2AM9).

No	Compounds	$\Delta G(\text{kcal/mol})$	Inhibition Constant (nM)	Amino Acid Interaction		
				Hydrogen Bond	Van der waals Bond	Others
1	Bicalutamide	-10.11	39.03 nM	752-Arg	-	Halogen: 745-Met; Pi-pi T-Shaped: 764-Phe; Alkyl/Pi-Alkyl: 895-Met, 701-Leu, 704-Leu, 707-Leu, 749-Met, 746-Val. Halogen: 745-Met; Pi-pi T-Shaped: 764-Phe; Alkyl/Pi-Alkyl: 895-Met, 701-Leu, 704-Leu, 707-Leu, 749-Met, 746-Val. Pi-Alkyl/Alkyl: 880-Leu, 873-Leu, 876-Phe, 701-Leu, 742-Met, 741-Trp, 704-Leu, 764-Phe, 707-Leu, 780-Met. Pi-Alkyl/Alkyl: 749-Met, 707-Leu, 764-Phe, 742-Met, 704-Leu, 891-Phe, 780-Met, 876-Phe, 701-Leu, 880-Leu., 895-Met.
2	Flutamide	-7.69	2.31×10^3 nM	752-Arg	-	Halogen: 745-Met; Pi-pi T-Shaped: 764-Phe; Alkyl/Pi-Alkyl: 895-Met, 701-Leu, 704-Leu, 707-Leu, 749-Met, 746-Val. Pi-Alkyl/Alkyl: 880-Leu, 873-Leu, 876-Phe, 701-Leu, 742-Met, 741-Trp, 704-Leu, 764-Phe, 707-Leu, 780-Met. Pi-Alkyl/Alkyl: 749-Met, 707-Leu, 764-Phe, 742-Met, 704-Leu, 891-Phe, 780-Met, 876-Phe, 701-Leu, 880-Leu., 895-Met.
3	Abiraterone	-12.33	912.74×10^{-3} nM	711-Gln, 745-Met, 752-Arg, 705-Asn.	-	Halogen: 745-Met; Pi-pi T-Shaped: 764-Phe; Alkyl/Pi-Alkyl: 895-Met, 701-Leu, 704-Leu, 707-Leu, 749-Met, 746-Val. Pi-Alkyl/Alkyl: 880-Leu, 873-Leu, 876-Phe, 701-Leu, 742-Met, 741-Trp, 704-Leu, 764-Phe, 707-Leu, 780-Met. Pi-Alkyl/Alkyl: 749-Met, 707-Leu, 764-Phe, 742-Met, 704-Leu, 891-Phe, 780-Met, 876-Phe, 701-Leu, 880-Leu., 895-Met.
4	Ursolic Acid	-6.13	32.35×10^3 nM	711-Gln, 745-Met, 873-Leu.	-	Halogen: 745-Met; Pi-pi T-Shaped: 764-Phe; Alkyl/Pi-Alkyl: 895-Met, 701-Leu, 704-Leu, 707-Leu, 749-Met, 746-Val. Pi-Alkyl/Alkyl: 880-Leu, 873-Leu, 876-Phe, 701-Leu, 742-Met, 741-Trp, 704-Leu, 764-Phe, 707-Leu, 780-Met. Pi-Alkyl/Alkyl: 749-Met, 707-Leu, 764-Phe, 742-Met, 704-Leu, 891-Phe, 780-Met, 876-Phe, 701-Leu, 880-Leu., 895-Met.
5	Apigenin	-9.21	178.29 nM	711-Gln, 752-Arg, 705-Asn, 873-Leu.	-	Halogen: 745-Met; Pi-pi T-Shaped: 764-Phe; Alkyl/Pi-Alkyl: 895-Met, 701-Leu, 704-Leu, 707-Leu, 749-Met, 746-Val. Pi-Alkyl/Alkyl: 880-Leu, 873-Leu, 876-Phe, 701-Leu, 742-Met, 741-Trp, 704-Leu, 764-Phe, 707-Leu, 780-Met. Pi-Alkyl/Alkyl: 749-Met, 707-Leu, 764-Phe, 742-Met, 704-Leu, 891-Phe, 780-Met, 876-Phe, 701-Leu, 880-Leu., 895-Met.
6	Hispidulin	-9.43	123.12 nM	711-Gln, 752-Arg, 705-Asn, 873-Leu.	-	Halogen: 745-Met; Pi-pi T-Shaped: 764-Phe; Alkyl/Pi-Alkyl: 895-Met, 701-Leu, 704-Leu, 707-Leu, 749-Met, 746-Val. Pi-Alkyl/Alkyl: 880-Leu, 873-Leu, 876-Phe, 701-Leu, 742-Met, 741-Trp, 704-Leu, 764-Phe, 707-Leu, 780-Met. Pi-Alkyl/Alkyl: 749-Met, 707-Leu, 764-Phe, 742-Met, 704-Leu, 891-Phe, 780-Met, 876-Phe, 701-Leu, 880-Leu., 895-Met.
7	Myristic Acid	-7.09	6.38×10^3 nM	711-Gln, 752-Arg	-	Halogen: 745-Met; Pi-pi T-Shaped: 764-Phe; Alkyl/Pi-Alkyl: 895-Met, 701-Leu, 704-Leu, 707-Leu, 749-Met, 746-Val. Pi-Alkyl/Alkyl: 880-Leu, 873-Leu, 876-Phe, 701-Leu, 742-Met, 741-Trp, 704-Leu, 764-Phe, 707-Leu, 780-Met. Pi-Alkyl/Alkyl: 749-Met, 707-Leu, 764-Phe, 742-Met, 704-Leu, 891-Phe, 780-Met, 876-Phe, 701-Leu, 880-Leu., 895-Met.
8	Linolenic Acid	-8.79	357.94 nM	711-Gln, 752-Arg	-	Halogen: 745-Met; Pi-pi T-Shaped: 764-Phe; Alkyl/Pi-Alkyl: 895-Met, 701-Leu, 704-Leu, 707-Leu, 749-Met, 746-Val. Pi-Alkyl/Alkyl: 880-Leu, 873-Leu, 876-Phe, 701-Leu, 742-Met, 741-Trp, 704-Leu, 764-Phe, 707-Leu, 780-Met. Pi-Alkyl/Alkyl: 749-Met, 707-Leu, 764-Phe, 742-Met, 704-Leu, 891-Phe, 780-Met, 876-Phe, 701-Leu, 880-Leu., 895-Met.
9	9-hydroxy-cis-11-octadecenoic acid	-7.77	2.02×10^3 nM	787-Met, 704-Leu	-	Carbon Hydrogen Bond: 746-Val; Unfavorable Acceptor-Acc: 745-Met; Pi-Alkyl/Alkyl: 741-Trp, 742-Met, 873-Leu, 780-Met, 764-Phe, 707-Leu Pi-Alkyl/Alkyl: 745-Met, 742-Met, 749-Met, 873-Leu, 746-Val, 764-Phe, 707-Leu, 704-Leu.
10	Lignoceric Acid	-7.31	4.35×10^3 nM	-	-	Carbon Hydrogen Bond: 746-Val; Unfavorable Acceptor-Acc: 745-Met; Pi-Alkyl/Alkyl: 741-Trp, 742-Met, 873-Leu, 780-Met, 764-Phe, 707-Leu Pi-Alkyl/Alkyl: 745-Met, 742-Met, 749-Met, 873-Leu, 746-Val, 764-Phe, 707-Leu, 704-Leu.

No	Compounds	$\Delta G(\text{kcal/mol})$	Inhibition Constant (kl)	Amino Acid Interaction		
				Hydrogen Bond	Van der waals Bond	Others
11	Oleanolic Acid	-5.63	$75.14 \times 10^3 \text{ nM}$	873-Leu	-	Pi-Alkyl/Alkyl: 745-Met, 707-Leu, 749-Met, 764-Phe, 704-Leu, 880-Leu, 701-Leu, 889-Val, 876-Phe, 891-Phe; Unfavorable Bump: 711-Gln; Unfavorable Donor-Donor: 752-Arg Alkyl: 701-Leu, 873-Leu, 704-Leu, 895-Met, 742-Met, 745-Met.
12	Linoleic Acid	-8.46	625.23 nM	711-Gln, 764-Phe	-	880-Leu, 877-Thr, 891-Phe, 701-Leu, 876-Phe, 873-Leu, 780-Met, 746-Val, 749-Met, 707-Leu, 752-Arg, 745-Met, 708-Gly, 742-Met, 704-Leu, 741-Trp, 895-Met
13	Aucubin	-7.27	$4.72 \times 10^3 \text{ nM}$	705-Asn, 711-Gln	-	Pi-alkyl: 764-Phe
14	Asperuloside	-8.84	332.57 nM	704-Leu	-	Carbon Hydrogen Bond: 705-Asn; Sulfur-X: 742-Met; Pi-Alkyl/Alkyl: 873-Leu, 876-Phe, 701-Leu, 780-Met. Pi-Alkyl/Alkyl: 787-Met, 746-Val, 749-Met, 764-Phe, 742-Met, 742-Trp, 745-Met, 873-Leu, 876-Phe, 701-Leu, 880-Leu, 704-Leu, 895-Met.
15	Arachidic Acid	-8.13	$1.09 \times 10^3 \text{ nM}$	711-Gln, 752-Arg	-	Pi-Alkyl/Alkyl: 895-Met, 873-Leu, 742-Met, 764-Phe, 701-Leu, 704-Leu, 707-Leu
16	Stearic Acid	-8.07	$1.22 \times 10^3 \text{ nM}$	711-Gln, 745-Met, 752-Arg.	-	

bonding, and the similarity of amino acid residues of each test ligand, shown in Table 4. The affinity of the ligand to the receptor is determined by the value of binding energy (ΔG) and constant inhibition (Kim and Skolnick, 2008). Strong complex-forming bonds are characterized by low G values, low inhibition constants, and many hydrogen bonding interactions (Tambunan, *et al.*, 2011). The negative sign of the Gibbs free energy value

and the smaller the value of the inhibition constant indicates that the complex formed between the ligand and the standard is powerful.

Bicalutamide, Flutamide, and Abiraterone were employed as reference ligands in this research. The medication has been approved for the treatment of prostate cancer. However, its use can result in mutations that can indicate drug resistance. Bicalutamide induces a AR W741C/L mutation,

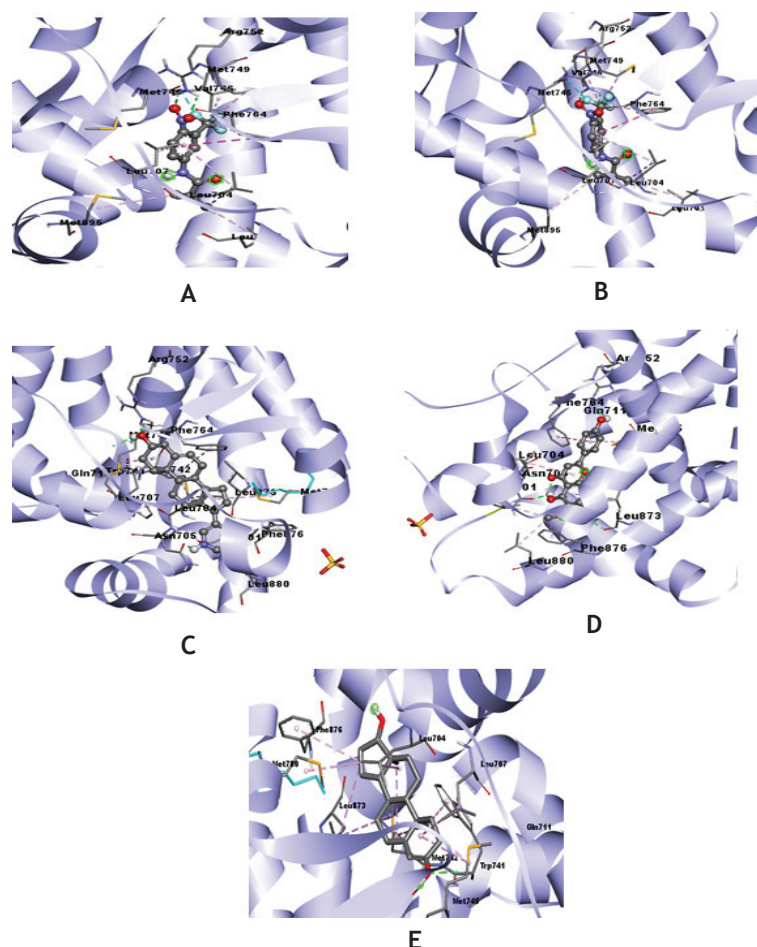


Figure 4. Molecular interaction reference ligand. A. Bicalutamide-AR(2AM9), B. Flutamide-AR(2AM9), C. Abiraterone-AR(2AM9); and Test Ligand, D. Hispidulin-AR(2AM9); and Native Ligand, E. Testosterone-AR(2AM9).

flutamide causes an AR T877A mutation, and abiraterone causes CYP3A overexpression in the intratumoral area (Balbas, *et al.*, 2013; Cai, *et al.*, 2011). This encourages researchers to look for alternative therapies, one of which is the development of herbal medicines. *Plantago major* L. may be an option because of its reported cancer activity and low toxicity (Kartini, *et al.*, 2017; BPOM, 2010). Based on the test results, no test compound has a higher affinity than testosterone which acts as an androgen receptor agonist. Still, the reference ligand abiraterone (-12.33 kcal/mol) has a lower ΔG than the natural testosterone ligand (-11.98 kcal/mol). Visualization of the molecular interactions between the reference ligand-AR(2AM9) is shown in Figure 4.

Based on the docking results obtained, it is known that the hispidulin compound gave the most negative ΔG value (-9.43 kcal/mol) and the lowest inhibition constant compared to other test ligand compounds. This means that hispidulin has the highest affinity for the androgen receptor. Moreover, the visualization results show that hispidulin has hydrogen bonds in common with 711-Gln and 705-Asn, which are the primary amino acid residues of the androgen receptor responsible for agonist activity via modulation of the 'active conformation' that determines the receptor for coactivators binding to the activation function 2 (AF2) region, a hydrophobic surface consisting of helices 3, 4, and 12 located in LBD (Tan, *et al.*,

2015). Visualization of the molecular interaction of hispidulin-AR (2AM9) is shown in Figure 4. Test ligands with amino acid residues and hydrogen bonds close to natural ligands show a similar type of interaction and, in this case, illustrate the similarity of activity (Cosconati, *et al.*, 2010).

Hispidulin complied with all the required Lipinski rules (RO5) and ADMET, shown in Tables 1 and 2. Hispidulin was predicted to have an LD₅₀ value of 4000 mg/kg with a relatively safe toxicity level of 5. The results of cytotoxic screening have reported that hispidulin has anticancer activity against prostate cancer cell lines and pancreatic cancer cell lines. Prostate cancer cell lines and Pancreatic cancer cell lines can be one indicator of the presence of CRPC (Jacob, *et al.*, 2010; Sak, 2014). The administration of hispidulin (10 µM and 50 µM) was reported to significantly inhibit prostate cancer cell migration (Du145, VCaP); the rate of apoptosis increased with the administration of hispidulin (Wang, *et al.*, 2021). In the PANC-1 cell pancreatic tumor xenograft model, administration of Hispidulin (20 mg kg⁻¹ day⁻¹ S.C.) significantly suppressed tumor growth and volume with little change in mouse weight (He, *et al.*, 2011). This research is still only a hypothesis as the first step in drug discovery. Further computational research is needed to strengthen the theory before conducting experimental studies (*in vitro* and *in vivo*).

CONCLUSION

Based on this study, hispidulin has the highest potential as an anti-androgen with binding energy (-9.43 kcal/mol) close to natural ligands (testosterone). This anti-androgen activity was hypothesized from the similarity of hydrogen bonds with 705-Asn and 711-Gln as key AR residues present in hispidulin.

ACKNOWLEDGEMENT

This research is part of a series of drug discovery and development research conducted at

the Faculty of Pharmacy, Padjadjaran University. The author thanks the laboratory assistant which has guided this research.

REFERENCES

- Adom, M.B., Taher, M., Mutalabisin, M.F., Amri, M.S., Kudos, MDA., Sulaiman, MWA., *et al.*, 2017, Chemical constituents and medical benefits of *Plantago major*, *Biomed Pharmacother*, **96**, 348-360.
- Atkovska, K., Samsonov S.A., Paszkowski-Rogacz, M., and Pisabarro, M.T., 2014 Multipose Binding in Molecular Docking, *Int J Mol Sci.*, **15**(2), 2622-2645.
- Balbas, M.D., Evans, M.J., Hosfield, D.J., Wongvipat, J., Arora, V.K. Watson, P.A., *et al.*, 2013, Overcoming mutation-based resistance to antiandrogens with rational drug design, *eLife*, **2**(2).
- Bissantz, C., Folkers, G., and Rognan, D., 2000, Protein-based virtual screening of chemical databases. 1. Evaluation of different docking/scoring combinations, *Journal of medicinal chemistry*, **43**(25), 4759-4767.
- Bohnert, T., and Gan, L., 2013, Plasma Protein Binding: from Discovery to Development INTRODUCTION TO FREE DRUG THEORY—WHY IS PLASMA PROTEIN BINDING, (March), 1-42.
- BPOM, 2010, Acuan Sediaan Herbal Volume Kelima Edisi Pertama. 1st ed. Jakarta: Direktorat Obat Asli Indonesia BADAN POM RI.
- Brito, M.A., and Araújo De Brito, M., 2011, Pharmacokinetic study with computational tools in the medicinal chemistry course, *Brazilian Journal of Pharmaceutical Sciences*, **47**(4), 797-805.
- Bronowska, A.K., 2011, Thermodynamics of Ligand-Protein Interactions: Implications for Molecular Design, Thermodynamics-Interaction Studies-Solids, Liquids and Gases.
- Cai, C., Chen, S., Ng, P., Buble, G.J., Nelson, P.S., Mostaghel, E.A., *et al.*, 2011, Intratumoral De Novo Steroid Synthesis Activates Androgen Receptor in Castration-Resistant Prostate Cancer and is Upregulated by Treatment with

- CYP17A1 Inhibitors, *Cancer Research*, **71**(20), 6503-6513.
- Cheng, F., Li, W., Zhou, Y., Shen, J. Wu, Z., Liu, G., et al., 2012, AdmetSAR: A comprehensive source and free tool for assessment of chemical ADMET properties, *Journal of Chemical Information and Modeling*, **52**(11), 3099-3105.
- Clark, A.M., and Labute, P., 2007, 2D depiction of protein-ligand complexes, *Journal of chemical information and modeling*, **47**(5), 1933-1944.
- Cosconati, S., Forli, S., Perryman, Harris, R., Goodsell, D.S., and Olson A.J., 2010, Virtual Screening with AutoDock: Theory and Practice, *Expert opinion on drug discovery*, **5**(6), 597-607.
- Dieter, S., 2018, What is the meaning of "A compound is carcinogenic"?, *Toxicology Reports*, **5**, 504-511.
- Forli, S., Huey, R., Pique, M.E., Sanner, M.F., Goodsell, D.S., and Olson, A.J., 2016, Computational protein-ligand docking and virtual drug screening with the AutoDock suite, *Nature Protocols*, **11**(5), 905-919.
- Fujita, K., and Nonomura, N., 2019, Role of androgen receptor in prostate cancer: A review, *World Journal of Men's Health*, **37**(3), 288-295.
- Gowthaman, U., Jayakanthan, M., and Sundar, D., 2008, Molecular docking studies of dithionitrobenzoic acid and its related compounds to protein disulfide isomerase: Computational screening of inhibitors to HIV-1 entry, *BMC Bioinformatics*, **9**(Suppl.12), 1-10.
- He, L., Wu, Y., Wang, L.L.J., Wu, Y., Chen, Y., Yi, Z., et al., 2011 Hispidulin, a small flavonoid molecule, suppresses the angiogenesis and growth of human pancreatic cancer by targeting vascular endothelial growth factor receptor 2-mediated PI3K/Akt/mTOR signaling pathway, *Cancer Science*, **102**(1), 219-225.
- Jacob, J., Chargari, C., Bauduceau, O., Fayolle, M., Ceccaldi, B., Prat, F., et al., 2010, Pancreatic metastasis from prostate cancer, *Case Reports in Medicine*, **2010**, 826273.
- Kartini, Piyaviriyakul, S., Thongpraditchote, S., Siripong, P., and Vallisuta, O., 2017, Effects of *Plantago major* Extracts and Its Chemical Compounds on Proliferation of Cancer Cells and Cytokines Production of Lipopolysaccharide-activated THP-1 Macrophages, *Pharmacognosy Magazine*, **13**(51), 393-399.
- Kim, R., and Skolnick, J., 2008, Assessment of Programs for Ligand Binding Affinity Prediction, *Journal of computational chemistry*, **29**(8), 1316-1331.
- Kontoyianni, M., McClellan, L.M., and Sokol, G.S. 2004, Evaluation of docking performance: comparative data on docking algorithms, *Journal of medicinal chemistry*, **47**(3), 558-565.
- Larregieu, C.A., and Benet, L.Z., 2014, Distinguishing between the Permeability Relationships with Absorption and Metabolism To Improve BCS and BDDCS Predictions in Early Drug Discovery, *Mol Pharm.*, **11**(4), 1335-1344.
- Lipinski, C.A., Lombardo, F., Dominy, B.W., and Feeney, P.J., 1997, Experimental and computational approaches to estimate solubility and permeability in drug discovery and development settings, *Advanced Drug Delivery Reviews*, **23**(1-3), 3-25.
- Lipinski, C.A., 2004, Lead- and drug-like compounds: the rule-of-five revolution, *Drug discovery today. Technologies*, **1**(4), 337-341.
- Mannhold, R., 2008, Molecular drug properties : measurement and prediction, *Journal of Medicinal Chemistry*. Weinheim: Wiley-VCH.
- Mohamed, Kobeasy, I., Osama, Abdel-Fatah, M., El-Salam, S.M.A., and Mohamed, Z.E-O.M., 2011, Biochemical studies on *Plantago major* L. and *Cyamopsis tetragonoloba* L., *International Journal of Biodiversity and Conservation*, **3**(3), 83-91.
- Moradi, S., Kelarjani, M.K., and Shokri, V., 2021, Prostate cancer as a multifactorial disorder; an overview of different sides of disease, *Central Asian Journal of Medical and Pharmaceutical Sciences Innovation*, **3**, 143-150.
- Peng, C.C., Chen, C-Y., Chen, C-R., Chen, C-J.,

- Shen, K-H., Chen, K-C., *et al.*, 2019, Renal Damaging Effect Elicited by Bicalutamide Therapy Uncovered Multiple Action Mechanisms as Evidenced by the Cell Model, *Scientific Reports*, **9**, 3392.
- Pereira de Jésus-Tran, K., Cote, P-L., Cantin, L., Blanchet, J., Labrie, F., and Breton, R., 2006, Comparison of crystal structures of human androgen receptor ligand-binding domain complexed with various agonists reveals molecular determinants responsible for binding affinity, *Protein science: a publication of the Protein Society*, **15**(5), 987-999.
- Pratama, M.R.F., 2015, Molecular Docking of Anti-cancer Agents: Artemisinin and Derivatives as HER2 Inhibitor, Proceeding Sari Mulia International Conference on Health and Sciences, (December), pp. 155-168.
- Rendi, I.P., Maranata, J., Chaerunisa, H., Nugraheni, N., and Alfathonah, S.S., 2021, Molecular Docking of Compounds in *Moringa oleifera* Lam with Dipeptidyl Peptidase-4 Receptors as Antidiabetic Candidates, *Jurnal Farmasi dan Ilmu Ke-farmasian Indonesia*, **8**(3), 242-249.
- Rice, M.A., Malhotra, S.V., and Stoyanova, T., 2019, Second-generation antiandrogens: From discovery to standard of care in castration resistant prostate cancer, *Frontiers in Neurology*, **10**, 801.
- Roy, K., Kar, S., and Das, R.N., 2015, Computational Chemistry, Understanding the Basics of QSAR for Applications in Pharmaceutical Sciences and Risk Assessment, 151-189.
- Sak, K., 2014, Cytotoxicity of dietary flavonoids on different human cancer types, *Pharmacognosy Reviews*, **8**(16), 122-146.
- Scher, H.I., and Sawyers, C.L., 2005, Biology of progressive, castration-resistant prostate cancer: directed therapies targeting the androgen-receptor signaling axis, *Journal of clinical oncology : official journal of the American Society of Clinical Oncology*, **23**(32), 8253-8261.
- Siegel, R.L., Milleer, K.D., Fuch, H.E., and Jemal, A., 2021, Cancer Statistics, 2021, *CA: A Cancer Journal for Clinicians*, **71**(1), 7-33.
- Sung, H., Ferlay, J., Siegel, R.L., Laversanne, M., Soerjomataram, I., Jemal, A., *et al.*, 2021 Global Cancer Statistics 2020: GLOBOCAN Estimates of Incidence and Mortality Worldwide for 36 Cancers in 185 Countries, *CA: a cancer journal for clinicians*, **71**(3), 209-249.
- Tambunan, U.S.F., Apriyanti, N., Parikesit, A.A., Chua, W., and Wuryani, K., 2011, Computational design of disulfide cyclic peptide as potential inhibitor of complex NS2B-NS3 dengue virus protease, *African Journal of Biotechnology*, **10**(57), 12281-12290.
- Tan, M.H.E., Li, J., Xu, H.E., Melcher, K., and Yong, E-L., 2015, Androgen receptor: structure, role in prostate cancer and drug discovery, *Acta pharmacol Sin.*, **36**(1), 3-23.
- Tsao, P.A., Estes, J.P., Griggs, J., Smith, D.C., and Caram, M.E.V., 2019, Cardiovascular and Metabolic Toxicity of Abiraterone in Castration-resistant Prostate Cancer: Post-marketing Experience, *Clinical genitourinary cancer*, **17**(3), e592-e601.
- Villanueva-Paz, M., Moran, L., Lopez-Alcantara, N., Freixo, C., Andrade, R.J., Lucena, M.I., *et al.*, 2021, Oxidative stress in drug-induced liver injury (Dili): from mechanisms to biomarkers for use in clinical practice, *Antioxidants*, **10**(3), 390.
- Wang, Y., Guo, S., Jia, Y., Yu, X., Mou, R., and Li, X., 2021, Hispidulin inhibits proliferation, migration, and invasion by promoting autophagy via regulation of PPAR γ activation in prostate cancer cells and xenograft models, *Bioscience, biotechnology, and biochemistry*, **85**(4), 786-797.
- WHO, 2021a, Cancer Incident in Indonesia, Source: Globocan 2020, International Agency for Research on Cancer WHO.
- WHO, 2021b, World Factsheets, Source: Globocan 2020, International Agency for Research on Cancer WHO.